Orange-G as potential corrosion inhibitor for mild steel in acid medium.

G.V. Megha[1¥*], R.S. Vishwanath[2], D.R. Thanushre[3] , T. Naveen kumar[4], K. Upendranath[5¥*],.

[1]*Department of PG Chemistry, Surana College, Autonomous, South-end Circle, Bangalore, Karnataka, India-560004*

[2]*Centre for Research in Functional Materials (CRFM), JAIN (Deemed-to-be University), Jain Global Campus, Bengaluru 562-112, India*

[3]*Department of PG Chemistry, Surana College, Autonomous, South-end Circle, Bangalore, Karnataka, India-560004*

[4]*Department of PG Chemistry, Surana College, Autonomous, South-end Circle, Bangalore, Karnataka, India-560004*

[5]*Centre for Research in Functional Materials (CRFM), JAIN (Deemed-to-be University), Jain Global Campus, Bengaluru 562-112, India.*

Corresponding authors*: *K. Upendranath
Megha G V

Abstract

Organic dyes are frequently employed as corrosion inhibitors for metals and alloys in severe conditions. Nonetheless, their stability, longevity, and efficiency often exhibit limitations, necessitating an investigation of better alternatives. This research examines the efficacy of Orange-G dye as a corrosion inhibitor for mild steel in a 0.5 M hydrochloric acid solution. The efficacy of inhibition was assessed using weight loss measurements analyzing the impacts of temperature (308-338K) and duration of exposure (3-6 h). Studies have suggested that Orange-G reduces anodic oxidation and cathodic reduction by creating a protective coating on the mild steel surface, therefore validating its function as a mixed-type inhibitor via potentiodynamic polarization. Increasing the dye concentration improved inhibitory effectiveness, reaching 73.4%, 76.2%, 81.5%, and 84.1% at 308 K. The corrosion rates were further examined with Arrhenius plots. Scanning electron microscope examination validated the establishment of a monolayer on the MS surface, by the Langmuir adsorption isotherm this confirms the Orange-G as an effective corrosion inhibitor for mild steel in acidic medium.

Keywords: Orange–G, Mild steel, Corrosion, Polarization, Weight loss. SEM

¥ = Authors are equally contributed

1. Introduction

Increase in demand for steel alloys in industrial sectors by using rapidly in the construction of oil pipelines and power station plants due to its higher mechanical strength [1, 2]. Steel alloys easily undergo corrosion when exposed to the environment and various attacks. Corrosion damages metal surfaces by a chemical or electrochemical interaction with an environment. [3, 4]. When pure metals are exposed to the environment, there is a loss of metal surface due to the transfer of electrons from the active region (anode) of the metal to an electron acceptor (cathode). This process involves ionic currents in the solution and electronic currents within the metal [5, 6]. The acidic solution is commonly employed to eliminate rust and scale in many industrial operations; hydrochloric acid (HCl) and sulfuric acid (H_2SO_4) are extensively utilized in the pickling of steel and ferrous alloys [7]. Several methods are known to prevent corrosion, likewise, metal coating, plating organic coatings, and organic dyes as corrosion inhibitors. Among the various methods to avoid or control degradation of the mild steel surface, corrosion inhibitors are one of the prevalent and best methods to use; adding an inhibitor in a small concentration to an environment effectively decreases and prevents the reaction with the environment. Corrosion can be minimized by a suitable strategy, which restricts, prevents, or even slows down the anodic or cathodic processes [8]. Corrosion inhibitors function by controlling corrosion through the suppression of either cathodic reduction or anodic oxidation. Most inhibitors are organic dye-based compounds containing conjugated systems, heteroatoms, and active functional groups such as nitro (NO_2) and hydroxyl (OH) groups. This is due to those being effective corrosion inhibitors due to their environmental availability, safety, and inexpensive [9].

Keeping in mind on above results, in this article, we are inspired to report on Orange-G (Orange-Gelb) as a synthetic azo dye as a corrosion inhibitor. A distinctive orange-red color demonstrates its inhibitory effect on mild steel in a 0.5M hydrochloric acid solution. The corrosion inhibition efficiency was assessed using weight loss measurements, while the inhibition effect was confirmed through scanning electron microscopy (SEM). Furthermore, thermodynamic parameters were extracted using adsorption isotherms derived from Arrhenius plots.

2. Materials and measurements

2.1. Experimental

All the chemicals and solvents are purchased commercially and used without further purification. Mild steel (MS) coupons were used for corrosion tests contained by wt % as 0.051 C: 0.023 Si: 0.005 P: 0.103 Al: 0.179 Mn: 0.023 S and iron (Fe). Before gravimetric measurements, the surface was cut into mechanical dimensions of 2 cm ×2 cm ×0.1 cm, respectively. Further, the specimens were polished using Silicon Carbide (200-600 grade) emery paper and cleaned with deionized water. Later, it was immersed in benzene and acetones for five seconds, then dried and washed with clean tissue paper; simultaneously, all the specimens were kept in desiccators until use. In the end, gravimetric measurement was estimated using analytical balance.

2.2. Inhibitor

The orange-G inhibitor was purchased from spectra chemicals and used without further purification. The preparation stock solution of orange-G inhibitor weighed the inhibitor compound of 0.001g and dissolved it in 100ml distilled water, which gave a 1ppm inhibitor solution. This stock solution was used to prepare different concentrations of orange-G for use in this experiment. The structure of Orange-G is shown in **Fig.1**.

As Shown in **Fig.1**. A Synthetic azo dye contains oxy & azo groups. The lone pair of electrons on the nitrogen and oxygen atom, along with π electrons in the dye compound co-ordinate to the active site, cause stronger interaction with the MS surface and can be used as a color marker to monitor the process of agarose gel electrophoresis, running approximately at the size of a 50 base pair DNA molecule and polyacrylamide gel electrophoresis. Orange-G shows only two colors in an aqueous solution: brilliant orange in neutral and acidic pH or red in pH greater than 9.

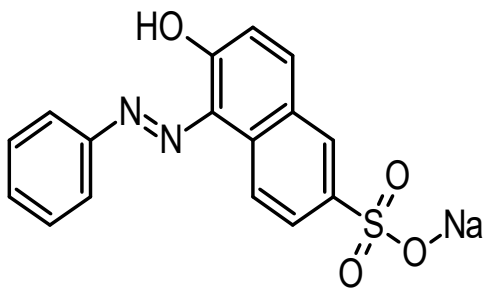

Fig. 1: Orange- G Dye compound

2.3. Gravimetric measurement

Gravimetric measurement was carried out in a boiling tube at 30 cm^3 with solution volume. The temperature of the environment is maintained by a thermostatically controlled water bath (Kemi) under aerated conditions. After the corrosion test in 0.5 M HCl with presence and absence inhibitor, the specimen was cleaned thoroughly using deionized water, then dried and weighed. Weight loss measurement of the specimen was estimated at a 3-6 h immersion period with a temperature range of 308, 318, 328, and 338 K. The doublet experiments were performed in each case, and the average mass loss was reported.

2.4 Scanning Electron Microscope

The SEM images were taken from a Zeiss electron microscope with a working voltage of 15kV and a working distance of 10mm. In SEM micrographs, the specimen was exposed to 0.5 m HCl for 3-6 hat optimized conditions with and without a corrosion inhibitor. SEM images of a polished specimen with and without inhibitors were collected.

3. Results and discussion

3.1. Mass loss measurements

3.1.1 effect of inhibitor efficiency (η %)

The values of the inhibition efficiency (η %) and corrosion rate in g cm^{-2} h^{-1} (C_R, Eq. 1 and 2) obtained from the mass loss method at different concentrations of Orange-G at different temperatures have been appended in **Table 1**.

$$C_R = \Delta W/St \qquad \textbf{Eq -1}$$

ΔW is the average weight loss (mg cm^{-2} h^{-1}), S is the surface area of the MS (cm^2), and t is the total time of immersion (h).

Inhibitor Efficiency (η %)

$$\eta\% = \frac{(C_R)_a - (C_R)_p}{(C_R)_a} \times 100 \qquad \textbf{Eq-2}$$

$(C_R)_a$ and $(C_R)_p$ are the corrosion rate in the presence and absence of inhibitors. The variation of corrosion rate with increasing temperature along with inhibitor concentrations is shown in **Fig. 2**.

The presence of π and a lone pair of electrons on the nitrogen and oxygen atoms on the inhibitor compound will coordinate with active sites, causing a strong interaction between the inhibitor

and metal surface. It has been noted that sulphur-containing organic compounds have better efficiency due to their electron donor capacity and easy polarizability [10, 11]. The percentage inhibition efficiency was found to increase with the increasing concentration of inhibitor and decreasing temperature.

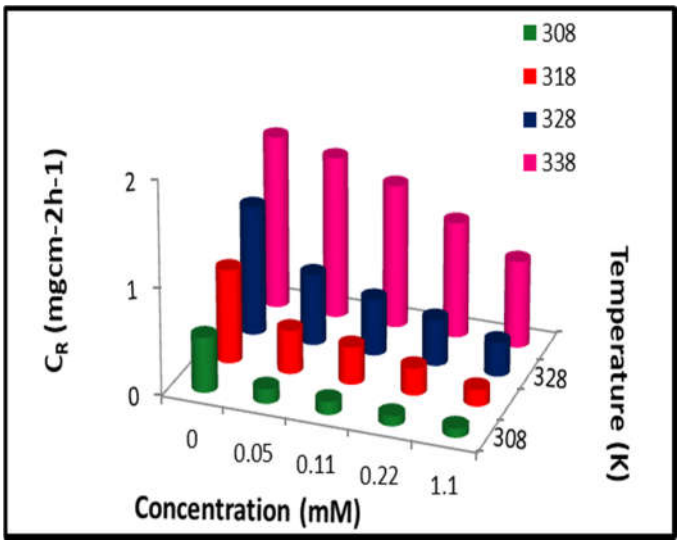

Fig. 2: Variation of corrosion rate with temperature and concentration of Orange-G.

Table.1

C_R and η% obtained from weight loss measurements of mild steel in 0.5 M HCl containing various concentrations of orange-G at different temperatures

C (mM)	C_R (mg cm^{-2} h^{-1})	η (%)	C_R (mg cm^{-2} h^{-1})	η (%)	C_R (mg cm^{-2} h^{-1})	η (%)	C_R (mg cm^{-2} h^{-1})	η (%)
	308 K		318 K		328 K		338 K	
Blank	0.516	-	0.883	-	1.224	-	1.65	-
0.05	0.137	73.4	0.407	53.9	0.671	45.2	1.537	6.8
0.11	0.122	76.2	0.350	60.2	0.529	56.7	1.455	11.8
0.22	0.095	81.5	0.254	71.2	0.435	64.4	1.394	15.5
1.10	0.082	84.1	0.157	82.2	0.318	74.0	1.360	17.6

3.2. Thermodynamic and activation parameters

The activation parameter plays a vital role in understanding the inhibitive mechanism of Orange-G. At different temperatures, increasing in temperature increases the corrosion rate and decreases in η%. Orange-G shows a very low inhibitive effect at a higher temperature. As the temperature increases, the time gap between the adsorption of dye molecules over the metal surface becomes shorter, so the surface stays exposed to the anodic environment for a longer

period; hence η% fails at elevated temperatures. The relation between corrosion rate (C_R) and temperature (T) can be expressed by the following Arrhenius **Eq. 3.**

$$C_R = Aexp(-\frac{Ea}{RT}) \qquad \textbf{Eq-3}$$

The inhibitor was calculated from the plots of the logarithm of C_R versus 1/T as shown in **Fig. 3**. All the linear regression coefficients are close to 0.9, indicating that corrosion of MS in 0.5M hydrochloride acid can be explained using the kinetic model. The plots obtained are straight lines, and the slope of each straight line gives apparent activation energy.

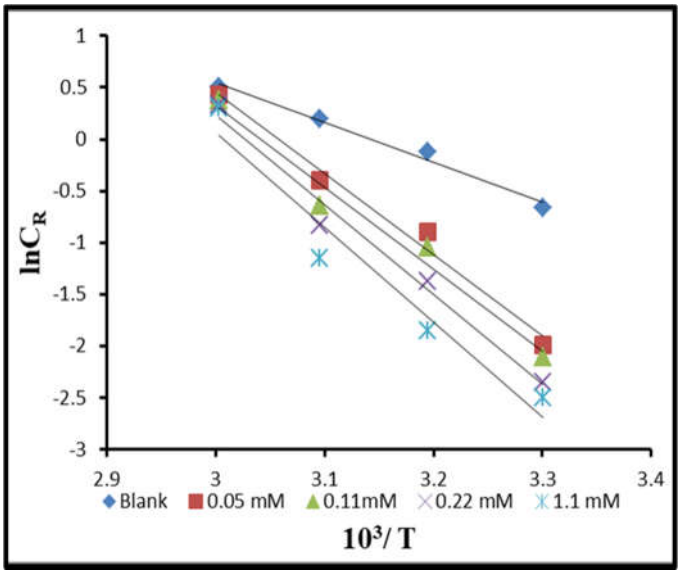

Fig. 3: Arrhenius plots of log C_R versus 1/T for mild steel in 0.5M HCl in the absence and presence of a different concentration of Orange–G.

Activation parameters for different concentrations of Orange-G have been summarized in **Table 2**. An increase in the value of activation energy (Ea) is due to a barrier formed by the inhibitor molecules on the mild steel surface. Enthalpy (ΔH_a^*) and entropy (ΔS_a^*) of activation were calculated using the alternative form of the Arrhenius **Eq. 4**.

$$C_R = \frac{RT}{Nh} exp\left(\frac{\Delta Sa*}{R}\right) \exp\left(-\frac{\Delta Ha*}{RT}\right) \qquad \textbf{Eq-4}$$

h is the plank constant, *N* is the Avogadro number, and *R* is the universal gas constant. From **Eq. 4**, a plot of log (C_R/T) versus 1/T gave a straight line with a slope of ($-\Delta H_a^*$ /2.303R) and an intercept of [log(R/Nh) + ΔS_a^*/2.303R] as shown in **Fig. 4**. Values of ΔH_a^* and ΔS_a^* are calculated with the help of plot. We observed the presence of an inhibitor produces higher values of ΔHa^* than those obtained for the absence of inhibitor in solution, indicating higher protection efficiency.

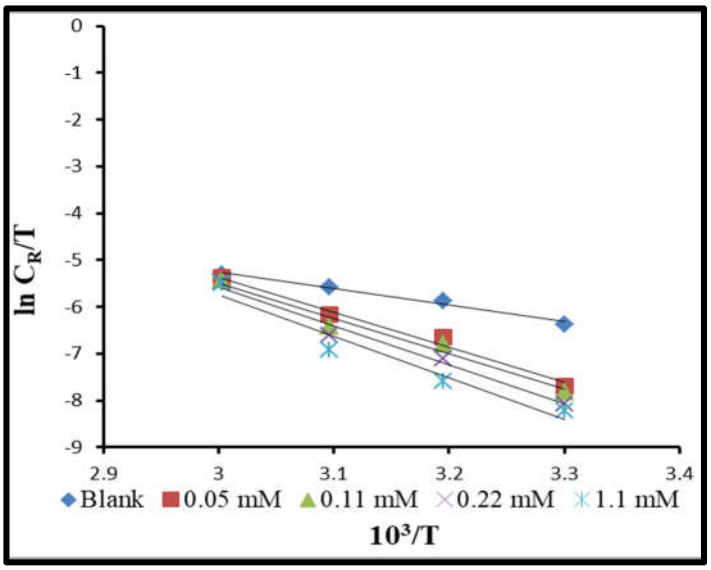

Fig. 4: Arrhenius plots of log C_R/T versus 1/T for mild steel in 0.5M HCl in the absence and presence of Orange-G.

The positive sign of a ΔH_a^* reflects the endothermic nature of the mild steel dissolution process, and it was slow in the presence of an inhibitor compound [12, 13]. **Fig. 5** shows that ΔH_a^* and E_a^* with a concentration of inhibitor are very similar in that an increase in the concentration of Orange-G compound increases in values of ΔH_a^* and Ea^* with concentration, continuously the reduction parameters and corrosion of mild steel were mainly decided by kinetic parameters of activation [14].

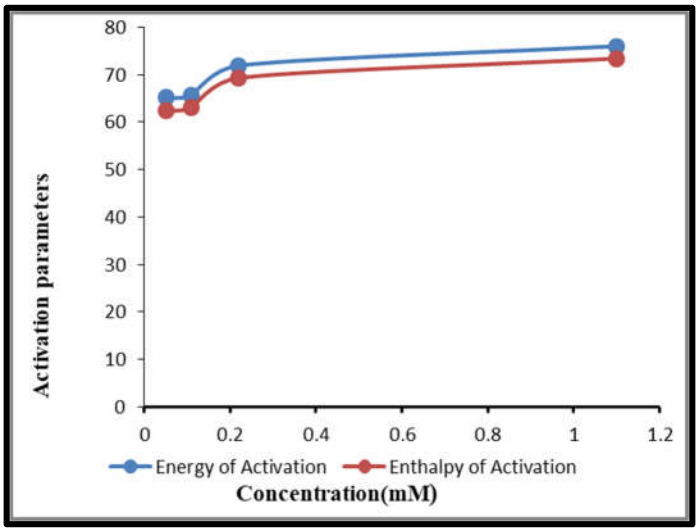

Fig. 5: Variation of activation parameters with concentration.

Table 2

Activation parameters of mild steel in 0.5 M HCl in the absence and presence of inhibitors at different concentrations of Orange-G

Concentration of Orange-G (mM)	E_a (kJ/mol)	A ($mg/cm^{-2}/h$)	ΔS_a^* (J/mol/K)	ΔH_a^* (kJ/mol)
Blank	32.1	1.86×10^{5}	-152.8	29.4
0.05	65.1	2.52×10^{10}	-54.6	62.4
0.11	65.7	2.74×10^{10}	-53.9	63.1
0.22	71.9	2.35×10^{11}	-36.1	69.3
1.10	76.0	8.78×10^{11}	-25.1	73.4

3.3 Effect of Immersion Time

The variation of inhibitor concentration changes in the immersion of time as shown in **Fig. 6**. The Inhibitor Efficiency (ŋ%) increases with immersion time increasing 3-6 h along with an increase in temperature to 308, 318, 328, and 338 K. The Inhibitor efficiency (ŋ%) increased with immersion time up to 10h and became constant. After 10h, there is the formation of the stable proactive layer at the metal-acid interface; hence the inhibitor efficiency becomes constant [15].

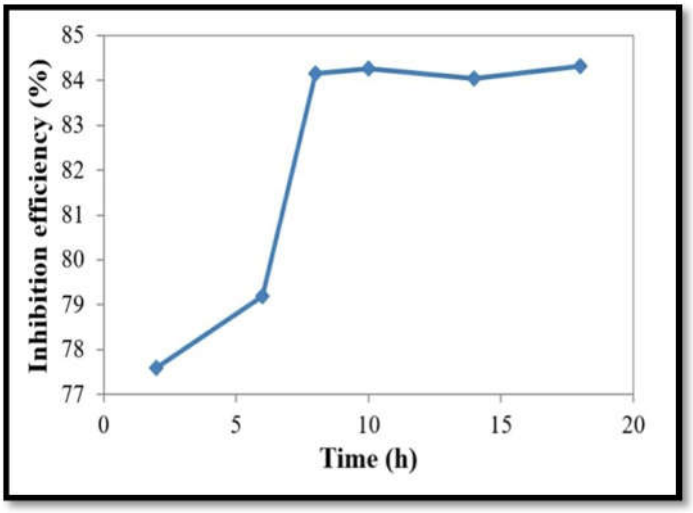

Fig. 6: Variation of inhibition efficiency with immersion time.

3.4. Adsorption isotherm

The interaction of inhibitor and metal surface is described by adsorption isotherm. The adsorption of inhibitor compound on the steel surface was either physisorption or chemisorption, and it's a substitution process where an exchange of adsorbed water molecules with organic dye compounds is performed. A linear relation between the degrees of the metal surface is covered by the inhibitor compound (Θ) and is dependent on inhibitor concentration (C). The classical adsorption model is applied to fit the surface coverage values at different inhibitor concentrations and temperatures. **Fig. 7** depicts the experimental results of C/Θ v/s C, giving straight lines as shown in good agreement with Langmuir's isotherm [16]. The strong correlation coefficient (R^2) suggests that the adsorption of inhibitor on the mild steel surface obeyed this isotherm [17]. Attempts were made to fit the data to different isotherms such as Langmuir, Freundlich, and Tempkin. We found that Langmuir adsorption isotherm was suitable to and given in **Eq-5** to this isotherm, Θ is related to the C and equilibrium constant adsorption K_{ads}.

$$\frac{C}{\theta} = \frac{1}{Kads} + C \qquad \textbf{Eq-5}$$

The equilibrium constant for the adsorption process from the Langmuir model adsorption isotherm model is related to the standard free energy of adsorption by the following expression.

$$\Delta G^{\circ}_{ads} = -RT \ln (55.5\ K_{ads}) \qquad \textbf{Eq- 6}$$

Here, R is the universal gas constant, temperature T, and 55.5 is the water concentration in the solution (mole /L^{-1}). The standard free energy of adsorption (ΔG_{ads}) that can characterize the interaction of adsorption molecules and mild steel surface was calculated by **Eq. 6.**

The enthalpy and entropy of adsorption (ΔH°_{ads} and ΔS°_{ads}) can be calculated with the help of Eq. 7 below, and the results are summarized in Table **3**.

$$\Delta G^{\circ}_{ads} = \Delta H^{\circ}_{ads} - T\Delta S^{\circ}_{ads} \qquad \textbf{Eq-7}$$

It is a straight-line form of the equation with the slope $-\Delta S^{\circ}_{ads}$ and intercepts ΔH°_{ads} as shown in **Fig. 8**.

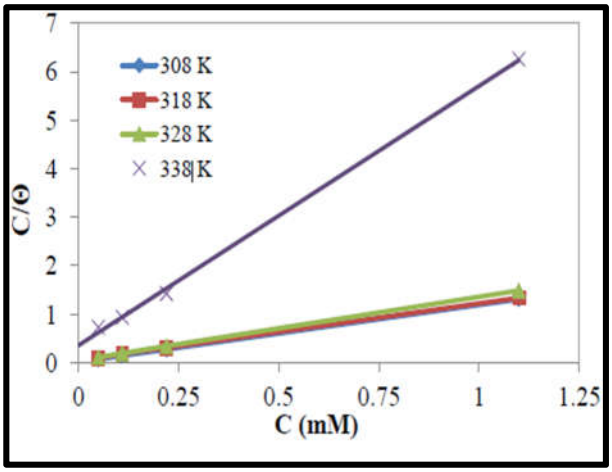

Fig. 7: Plot of Langmuir adsorption isotherm of inhibitor on mild steel in 0.5M HCl at different temperatures.

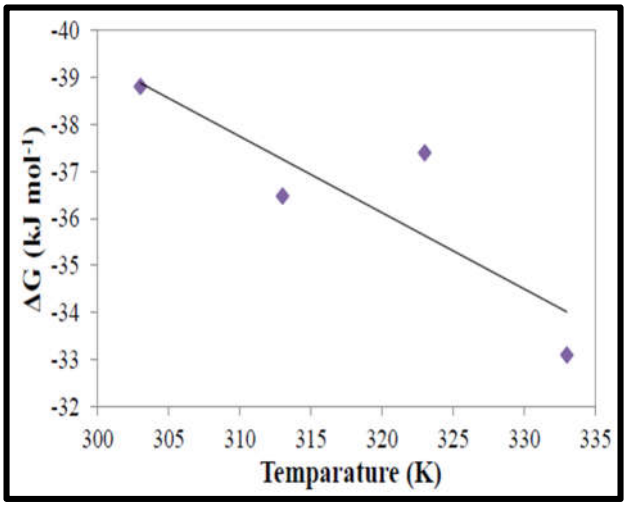

Fig. 8: Plot of Gibb's free energy versus absolute temperature.

Table 3

Thermodynamic adsorption parameter for adsorption of Orange-G on mild steel in 0.5M HCl at a different temperature from the Langmuir adsorption isotherm

T (K)	K_{ads} (L/mol)	R^2	ΔG°_{ads} (kJ/mol)	ΔH°_{ads} (kJ/mol)	ΔS°_{ads} (J/mol/K)
308	88496	1.0000	-38.8	-88.02	-162.2
318	22075	0.9998	-36.4		
328	20161	1.0000	-37.4		
338	2804	0.9998	-33.1		

3.5. Potentiodynamic polarisation.

The Potentiodynamic polarization curve for the Orange-G was recorded in 0.5 M HCl solution in the different concentrations 303 K as shown in **Fig. 9**. The various parameters like corrosion current density (I_{corr}), corrosion potential (E_{corr}), cathodic Tafel slope ($b\ c$), and anodic Tafel slope ($b\ a$) were calculated and are listed in **Table 4**. The corrosion current densities were calculated by extrapolating the linear parts of anodic and cathodic curves to the corresponding corrosion potential. The parallel cathodic Tafel curves showed that hydrogen evolution was activation-controlled, and the reduction mechanism was not affected by the presence of an inhibitor.

The inhibition efficiency can be calculated from the following equation:

$$IE(\%) = \frac{i°corr - icorr}{i°corr} \times 100 \qquad \textbf{Eq-8}$$

where i^o_{corr} and i_{corr} are the corrosion current densities in the absence and presence of the inhibitor, respectively.

Corrosion current remarkably decreased after the addition of Orange-G. The displacement of corrosion potential in all three cases is anodic. It is reported that if the displacement in E_{corr} is more than ± 85 mV relating to the corrosion potential of the blank, the inhibitor is either cathodic or anodic type. If the displacement in E_{corr} is less than ± 85 mV, the corrosion inhibitor may be regarded as a mixed type. In the present investigation, the displacements in E_{corr} were shown to be ±48 mV for Orange-G. So, all the studied inhibitors are of a mixed type, and orange-G is slightly more anodic. The electrochemical parameters such as corrosion potential (E_{corr}), corrosion current density (I_{corr}), Tafel slopes (ba, bc), and linear polarization are listed in **Table 4**.

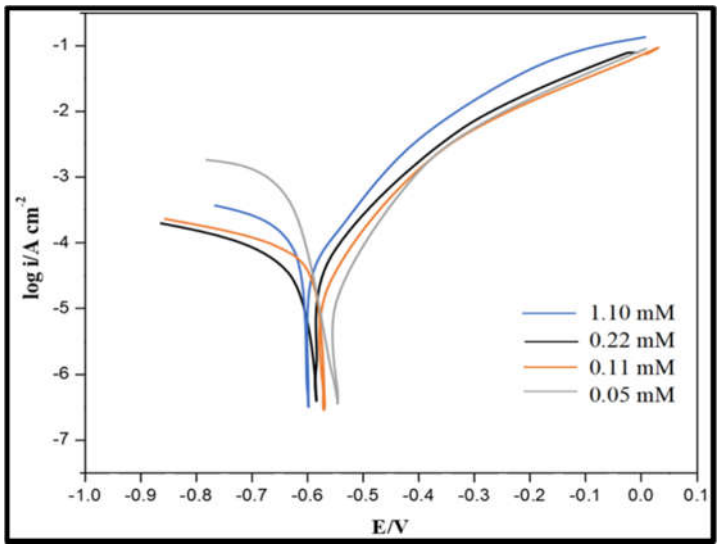

Fig. 9: Polarisation curves for MS in 0.5 M HCl containing different concentrations.

Table 4
Potentiodynamic polarization parameters for the corrosion of MS in 0.5 M HCl in the absence and presence of Orange-G at different concentrations.

Inhibitor	Concentration (mM)	E_{corr} (mV)	I_{corr} (mA cm^{-2})	b_c (mV dec^{-1})	b_a (mV dec^{-1})	Linear Polarization resistance (Ω cm^2)	IE (%)
Orange-G	Blank	-659	0.200	15.36	13.23	402	-
	0.05	-621	0.049	11.95	5.89	398.8	78.12
	0.11	-594	0.041	10.46	6.79	861.2	82.14
	0.22	-572	0.039	9.76	9.12	998.2	83.24
	1.10	-547	0.037	10.76	9.26	1024.9	84.16

3.7. Scanning Electron Microscope

In order to study the effect of morphological surface for mild steel from scanning electron micrograph (SEM) in 0.5M HCl solution at optimized condition without and with corrosion inhibitor after the immersion period 3-6 h time interval. In **Fig. 10** (a) the mild steel surface was covered with a high density of pits due to the absence of an inhibitor. Similarly, **Fig. 10** (c) shows no evidence of pitting but shows the formation of the thick film on the steel surface due to the presence of inhibitor, the micrograph. This result is due to the adsorption of inhibitor molecules around the pits in the presence of corrosion inhibitor to ensure a high degree of protection on mild steel surfaces and passive film blocks the active sites present on the iron surface.

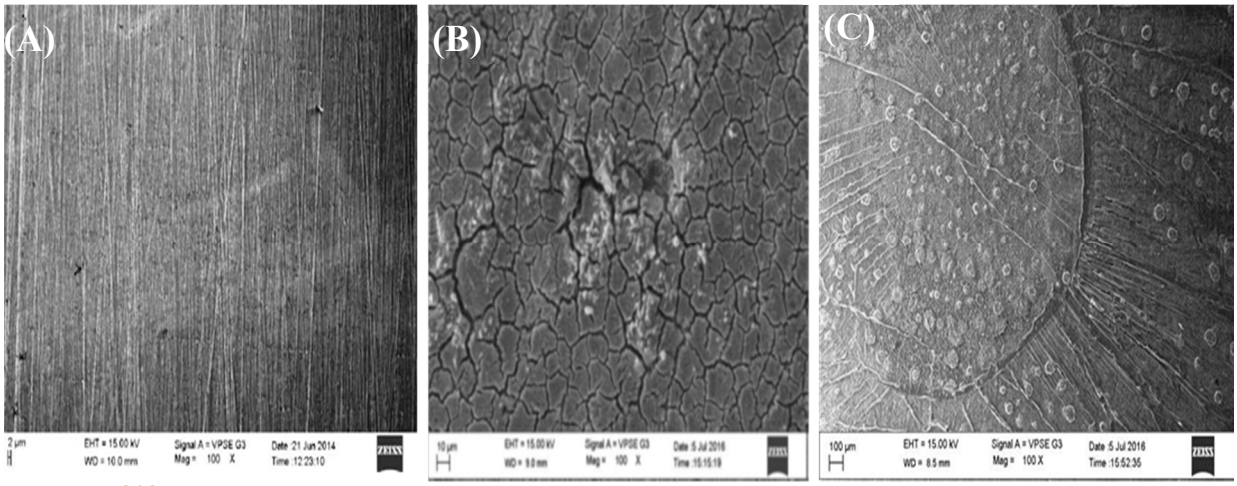

Fig. 10: SEM images of MS surface (**a**) polished (**b**) immersed in 0.5M HCl (**c**) immersed in 0.5M HCl in the presence of an optimum concentration of Orange-G.

4. Conclusion

In summary, Orange-G emerges as a good corrosion inhibitor to MS in 0.5 M HCl medium. The dye compound follows the Langmuir adsorption isotherm and inhibits the corrosion of MS by forming complex, comprehensive adsorption, a mixture of physical and chemical adsorption. Polarisation studies confirm the inhibitor affects both the anodic and cathodic reactions at different temperatures. The formation of thick films on the surface by the SEM images; this leads to Orange-G acting as a good corrosion inhibitor over the MS surface.

5. Acknowledgment

G.V.M, D.R.T and T.N.K thanks to Dept. of Chemistry, Surana College, UK, and R.S.V thankful to the CRFM JAIN (Deemed-to-be University), India for the research facility. The authors are grateful to Saif, Karnataka Univerity Dharawad, and the University of Mysore for their spectral characterization facility.

6. Authors contribution

G. V. Megha, R.S. Vishwanath, and **D.R. Thanushre**, contributed substantially to designing, acquiring, analyzing, or interpreting data and writing. **K. Upendranath and T. Naveen Kumar** contributed Data curation, Formal analysis, Investigation, writing – reviewing, and editing.

Conflict of interest- No Conflict of interest

References

1) Salima K.A, Wassan B.A, Anees A.K, (2019) Int J Ind Chem 173:159-173.

2) Shemi A, Ouici H.B, Guendouzi A, Ferhat M, Benail O, Boudjellal F, (2021). J. Electrochem. Soc. 167:155508-155528.

3) Hameed B.M, Asaad H.S, Athraa H.M, Anees A.K, (2020) Chem. Afr. 3:263-276.

4) Salima K.A, Wassan B.A, Anees A.K, (2019)J. Bio. Tribo Corros. 5:15-25.

5) Muthamma K, Kumari P, Lavanya M, (2021) J. Bio. Tribo Corros 7:10-20.

6) Zachariah P.M, Keerthi R, Cyril A, J. Bincy, J. Sam (2020) Heliyon 6:2405-8440.

7) Sadoun A.M, Mohammed M.M, Elsayed E.M, Meselhy A.F, Omyma A. El-Kady J. (2021) Mat. Res. Tech. 9:4485-4498.

8) Cleophas A.L, Roland T.L, Abimbola P.P, (2019) Chem. Dat. Coll. **24**: 100280-100290.

9) Vandana S, Mahendra Y, Obot I.B, (2020) Colloids Surf. A Physicochem. Eng. As **599**: 124881-124893.

10) Chandrabhan V. Eno E.E, Quraishi M.A, (2020) J. Mol. Liq. 316:113874-113896.

11) Dheeraj S.C, Chandrabhan V, Quraishi M.A. (2020) J. Mol. Str. 1227:129374-12994.

12) A.F. Ahmed , A.K. Anees. L. Hongfang, F, Chaoyang, W, Junlei, A.F. Noor, and B.M. Hameed, J. Mol. Liq. **276**, 503 (2019). doi:10.1016/j.molliq.2018.12.015.

13) Merimi I, Benkaddour R, Lgaz H, Rezki N, Messali M, Jeffali F, Oudda H, Hammouti B, Mat. Tod. Proce. (2019)13:1008-1022

14) Dheeraj S.C, EL.M Khadija. Quraishi M.A, Lahcen B, (2020) Inte. J. Bio. Macr. 152: 234-241.

15) Chaitra T.K, Mohana K.N, Gurudatt D.M, Harmesh K, (2016) J. Taiwan Inst. Chem. Eng. **57**:521-531.

16) Chaitra T.K, Mohana K.N, Tandon C, Harmesh K. (2017) Arab. J. Basic Appl. Sci., **25** 45-55.

17) Pradeep K.C.B, Prashanth M.K, Mohana K.N, Jagadeesha M.B, Raghu M.S., Lokanath N.K, Yogesh K, (2020) Sur. and Int. 18:100446-100462.